

K^* photoproduction off the nucleon: $\gamma N \rightarrow K^* \Lambda$

Yongseok Oh*

*Department of Physics and Astronomy,
University of Georgia, Athens, Georgia 30602, U.S.A.*

Hungchong Kim†

*Department of Physics, Pohang University of
Science and Technology, Pohang 790-784, Korea*

Abstract

We study the photoproduction of $K^*(892)$ vector meson from both the charged and neutral reactions, $\gamma p \rightarrow K^{*+} \Lambda$ and $\gamma n \rightarrow K^{*0} \Lambda$. The production mechanisms that we consider include t -channel K^* , K , κ exchanges, s -channel nucleon diagram, and u -channel Λ , Σ , Σ^* diagrams. These could constitute important backgrounds for future investigation of “missing” resonances that can be searched for especially in these reactions. The t -channel K meson exchange is found to dominate the both reactions. The total and differential cross sections are presented together with some spin asymmetries.

PACS numbers: 13.60.Le, 13.60.-r, 13.60.Rj

*Electronic address: yoh@physast.uga.edu

†Electronic address: hungchon@postech.ac.kr

I. INTRODUCTION

The baryon spectra predicted by some quark models anticipate much more baryon resonances than the observed so far [1]. These “missing” resonances are expected to have rather small couplings to the πN channel, and various reaction mechanisms have been suggested to search for those resonances. One of them is to use photoproduction processes containing mesons other than pion(s) in the final state. For example, the photoproductions of $K\Lambda$ and $K\Sigma$ in the scattering off the nucleon may give us a clue on the existence of nucleon resonances that strongly couple to the kaon channel [2]. Vector meson photoproduction, $\gamma N \rightarrow VN$, where V stands for a vector meson (ρ, ω, ϕ), may also be useful to identify the missing resonances [3].

Recently, the interest in $K^*(892)$ vector meson photoproduction has been grown. This was initially triggered by the quark model which predicts that some nucleon resonances with higher mass can have sizable couplings with the K^* channel [2]. In addition, there are some preliminary experimental data from the CLAS Collaboration at Jefferson Lab. on the reactions of K^* photoproduction, i.e., $K^*\Sigma$ [4] and $K^*\Lambda$ [5] production. These experiments show that the total cross sections for K^* photoproduction, though small, are not so much suppressed than those for K photoproduction, and it leads to the conclusion that full coupled-channel analyses to search for the resonances should include the K^* channel as well [5]. Therefore, it is legitimate to study the production mechanisms of K^* photoproduction.

At present, theoretical works to understand the K^* photoproduction reactions are very limited. In Ref. [6], Zhao et al. studied $K^*\Sigma$ photoproduction from the proton targets using a quark model. This model is based on the quark-meson couplings whose coupling constants are assumed to be flavor-blind, which allows to use the values determined by other reactions. To implement the t -channel exchange contribution, the kaon exchange was considered. More accurate experimental data are needed to further test their model [4], and the other channels for K^* photoproduction like $K^*\Lambda$ were not considered.

In this paper, we investigate $K^*\Lambda$ photoproduction, $\gamma N \rightarrow K^*\Lambda$. The purpose of this study is to study the background production mechanisms that include t -channel K^* , K , and κ exchanges as well as s -channel nucleon and u -channel hyperon ($\Lambda, \Sigma, \Sigma^*$) diagrams. This can provide a platform for future investigation of nucleon resonances that can also contribute to this reaction near the threshold. Because of isospin, the s -channel Δ resonances are excluded, and this reaction has an advantage in the study of nucleon resonances. Our approach is based on the effective Lagrangians and similar to the work of Ref. [7]. By making use of the effective Lagrangians for K^* meson interactions, we evaluate the tree diagrams for K^* photoproduction. The coupling constants are constrained either by phenomenology or by quark model predictions when the experimental inputs are not available. One advantage of K^* photoproduction over K photoproduction is that it provides a chance to study the controversial scalar $\kappa(900)$ meson in the t -channel. Such a contribution is prohibited in kaon photoproduction since $\kappa \rightarrow K\gamma$ interaction is not allowed by angular momentum and parity consideration. We will see, however, that the $\kappa(900)$ meson exchange is suppressed in K^* photoproduction and it would be hard to identify the κ meson contribution in this reaction at present.

Since both the K^* and nucleon are isodoublets, we consider the following two reactions,

$$(I) : \gamma p \rightarrow K^{*+}\Lambda, \quad (II) : \gamma n \rightarrow K^{*0}\Lambda. \quad (1)$$

In the next Section, we develop our approach for K^* photoproduction. The effective La-

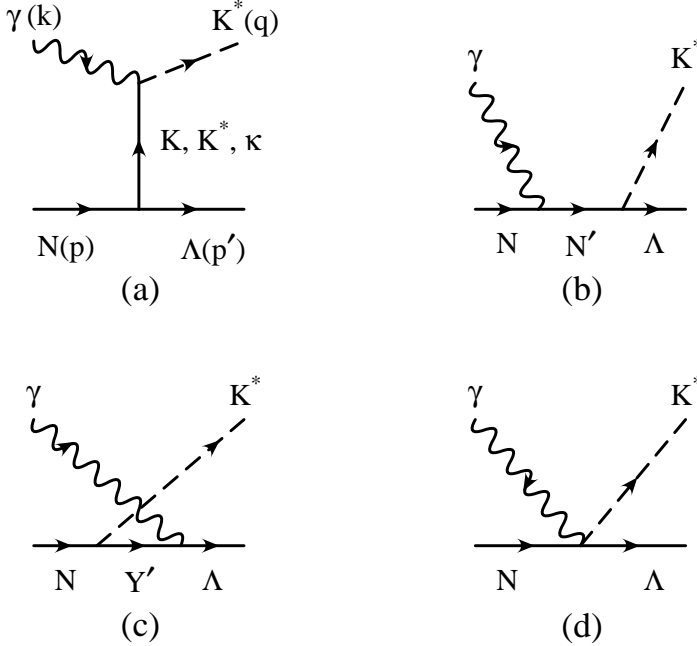


FIG. 1: Tree diagrams for $\gamma N \rightarrow K^* \Lambda$, which include (a) t -channel exchanges, (b) intermediate nucleon, (c) intermediate hyperon, and (d) contact diagrams.

grangians and their coupling constants are discussed in detail. Our results for cross sections and some spin asymmetries are given in Sec. III, and we summarize in Sec. IV.

II. MODEL

The tree diagrams we are considering are shown in Fig. 1, which also defines the momentum of each particle. In this calculation, we work with a model which includes (i) t -channel K , K^* , and κ exchanges, (ii) s -channel nucleon, and (iii) u -channel hyperon (Λ , Σ , Σ^*) terms. The contact term for the charged K^* photoproduction is included as well. Because of isospin conservation, the Δ resonances cannot contribute to this reaction. The production amplitude can then be written as

$$\mathcal{M} = \varepsilon_\nu^*(K^*) \bar{u}_\Lambda(p') \mathcal{M}^{\mu\nu} u_N(p) \varepsilon_\mu(\gamma), \quad (2)$$

where $\varepsilon^\mu(K^*)$ and $\varepsilon^\mu(\gamma)$ are the polarization vectors of K^* vector meson and the photon, respectively. The Dirac spinors of Λ and the nucleon are denoted by $u_\Lambda(p')$ and $u_N(p)$, respectively. Below we calculate $\mathcal{M}^{\mu\nu}$ for each channel.

A. t -channel K^* and K exchanges

Because of charge, the K^* exchange is present only for the charged K^* photoproduction, $\gamma p \rightarrow K^{*+} \Lambda$. The production amplitude is calculated from the following effective Lagrangians,

$$\mathcal{L}_{\gamma K^* K^*} = -ieA^\mu (K^{*-\nu} K_{\mu\nu}^{*+} - K_{\mu\nu}^{*-} K^{*+\nu}), \quad (3)$$

$$\mathcal{L}_{K^*N\Lambda} = -g_{K^*N\Lambda}\bar{N}\left(\gamma_\mu\Lambda K^{*\mu} - \frac{\kappa_{K^*N\Lambda}}{2M_N}\sigma_{\mu\nu}\Lambda\partial^\nu K^{*\mu}\right) + \text{H.c.}, \quad (4)$$

where A_μ is the photon field, $K_{\mu\nu}^{*\pm} = \partial_\mu K_\nu^{*\pm} - \partial_\nu K_\mu^{*\pm}$, and the isodoublets are defined by

$$K^* = \begin{pmatrix} K^{*+} \\ K^{*0} \end{pmatrix}, \quad N = \begin{pmatrix} p \\ n \end{pmatrix}. \quad (5)$$

We use the following coupling constants determined by the Nijmegen potential [8],

$$\begin{aligned} g_{K^*N\Lambda} &= -4.26, & \kappa_{K^*N\Lambda} &= 2.66 & \text{(NSC97a),} \\ g_{K^*N\Lambda} &= -6.11, & \kappa_{K^*N\Lambda} &= 2.43 & \text{(NSC97f).} \end{aligned} \quad (6)$$

The production amplitude then reads

$$\mathcal{M}_{K^*}^{\mu\nu} = \eta_{K^*} \frac{e}{(k-q)^2 - M_{K^*}^2} \Gamma_{K^*}^{\mu\nu\alpha}(k, q) P_{\alpha\beta}(k-q) \Gamma_{K^*N\Lambda}^\beta(q-k), \quad (7)$$

where $\eta_{K^*} = 1$ and 0 for the reaction (I) and (II) of Eq. (1), respectively, and

$$\begin{aligned} \Gamma_{K^*}^{\mu\nu\alpha}(k, q) &= 2q^\mu g^{\nu\alpha} - q^\alpha g^{\mu\nu} + k^\nu g^{\mu\alpha}, \\ P_{\alpha\beta}(k-q) &= g_{\alpha\beta} - \frac{(k-q)_\alpha (k-q)_\beta}{M_{K^*}^2}, \\ \Gamma_{K^*N\Lambda}^\mu(q-k) &= g_{K^*N\Lambda} \left[\gamma^\mu - \frac{i\kappa_{K^*N\Lambda}}{2M_N} \sigma^{\mu\nu} (q-k)_\nu \right]. \end{aligned} \quad (8)$$

The decay width of K^* , $\Gamma_{K^*} = 50.8$ MeV, is included by replacing M_{K^*} in the propagator by $M_{K^*} - i\Gamma_{K^*}/2$.

On the other hand, the t -channel kaon exchange is allowed for the both reactions. In this case, we have

$$\begin{aligned} \mathcal{L}_{\gamma KK^*} &= g_{\gamma KK^*}^0 \varepsilon^{\mu\nu\alpha\beta} \partial_\mu A_\nu (\partial_\alpha K_\beta^{*0} \bar{K}^0 + \partial_\alpha \bar{K}_\beta^{*0} K^0) \\ &\quad + g_{\gamma KK^*}^c \varepsilon^{\mu\nu\alpha\beta} \partial_\mu A_\nu (\partial_\alpha K_\beta^{*-} K^+ + \partial_\alpha K_\beta^{*+} K^-), \\ \mathcal{L}_{K N\Lambda} &= -ig_{K N\Lambda} \bar{N} \gamma_5 \Lambda K + \text{H.c.}, \end{aligned} \quad (9)$$

where K is the kaon iso-doublet, $K^T = (K^+, K^0)$. The coupling constants $g_{\gamma KK^*}$ can be calculated from the experimental data for $\Gamma(K^* \rightarrow K\gamma)$, which gives

$$g_{\gamma KK^*}^0 = -0.388 \text{ GeV}^{-1}, \quad g_{\gamma KK^*}^c = 0.254 \text{ GeV}^{-1}, \quad (10)$$

where the phases of the couplings are fixed from the quark model.

The coupling constant $g_{K N\Lambda}$ is obtained by using SU(3) flavor symmetry relation, which gives

$$g_{K N\Lambda} = -\frac{1}{\sqrt{3}}(1+2f)g_{\pi NN} = -13.24, \quad (11)$$

with $f = 0.365$ and $g_{\pi NN}^2/4\pi = 14.0$. In this work we employ the pseudoscalar coupling for this interaction. However, since the nucleon and Λ are on their mass-shell, it is equivalent to the pseudovector coupling. The production amplitude for the K exchange becomes

$$\mathcal{M}_K^{\mu\nu} = \frac{ig_{\gamma KK^*} g_{K N\Lambda}}{(k-q)^2 - M_K^2} \varepsilon^{\mu\nu\alpha\beta} k_\alpha q_\beta \gamma_5, \quad (12)$$

where $g_{\gamma KK^*} = g_{\gamma KK^*}^c$ for the reaction (I) and $g_{\gamma KK^*}^0$ for the reaction (II).

B. t -channel κ exchange

The scalar κ meson cannot couple to $K\gamma$ because of angular momentum and parity consideration and, as a result, the κ meson exchange is not present in kaon photoproduction. However, $\gamma K^* \kappa$ coupling is allowed and this provides us with a chance to study the controversial $\kappa(900)$ meson [9] in K^* photoproduction.

The effective Lagrangians for the scalar (and iso-doublet) κ meson interactions are given by

$$\begin{aligned}\mathcal{L}_{\gamma K^* \kappa} &= g_{\gamma K^* \kappa} A^{\mu\nu} \bar{\kappa} K_{\mu\nu}^* + \text{H.c.}, \\ \mathcal{L}_{\kappa N \Lambda} &= -g_{\kappa N \Lambda} \bar{N} \kappa \Lambda + \text{H.c.}\end{aligned}\quad (13)$$

where $A_{\mu\nu} = \partial_\mu A_\nu - \partial_\nu A_\mu$ and

$$\kappa = \begin{pmatrix} \kappa^+ \\ \kappa^0 \end{pmatrix}, \quad \bar{\kappa} = (\kappa^-, \bar{\kappa}^0). \quad (14)$$

The coupling constants are determined as follows. For $g_{\gamma K^* \kappa}$, we rely on the vector-meson dominance model in the SU(3) limit [10]. Here we briefly explain this model referring the details to Ref. [10]. The basic idea of this model is to start with the most general Lagrangian for the SVV interaction, where S stands for scalar meson nonet and V for vector meson nonet. Then the $\bar{q}q$ or \bar{q}^2q^2 nature of scalar mesons is revealed through the mixing angle between the scalar meson octet and scalar meson singlet. If the $\bar{q}q$ structure dominates the scalar meson wavefunction, then one would expect the mixing angle $\theta_S \simeq -20^\circ$, while the dominance of the tetraquark nature leads to $\theta_S \simeq -90^\circ$ [10]. The general form for the SVV interaction can then be written as [10]

$$\begin{aligned}\mathcal{L}_{SVV} &= \beta_A \epsilon_{abc} \epsilon^{a'b'c'} [V_{\mu\nu}]_{a'}^a [V_{\mu\nu}]_{b'}^b S_{c'}^c + \beta_B \text{Tr}(S) \text{Tr}(V^{\mu\nu} V_{\mu\nu}) \\ &\quad + \beta_C \text{Tr}(SV^{\mu\nu}) \text{Tr}(V_{\mu\nu}) + \beta_D \text{Tr}(S) \text{Tr}(V^{\mu\nu}) \text{Tr}(V_{\mu\nu}).\end{aligned}\quad (15)$$

Using the vector meson dominance hypothesis in the SU(3) limit, the $SV\gamma$ couplings of our concern can be expressed in terms of the above couplings β_i and the mixing angle, and we have

$$g_{\gamma K^* \kappa}^c = \frac{e}{g_\rho} \frac{2}{3} \beta_A, \quad g_{\gamma K^* \kappa}^0 = -\frac{e}{g_\rho} \frac{4}{3} \beta_A, \quad (16)$$

where $g_\rho = 4.04$ is the universal ρ meson coupling, and $g_{\gamma K^* \kappa}^c = g_{\gamma K^{*-} \kappa^+} = g_{\gamma K^{*+} \kappa^-}$ and $g_{\gamma K^* \kappa}^0 = g_{\gamma \bar{K}^{*0} \kappa^0} = g_{\gamma K^{*0} \bar{\kappa}^0}$. Since β_A is independent of the mixing angle θ_S [10], this shows that the coupling constants $g_{\gamma K^* \kappa}$ also do not depend on the mixing angle and, therefore, they are blind to whether the $\bar{q}q$ or \bar{q}^2q^2 nature dominates the scalar meson structure in the SU(3) limit. Note also that the ratio of the couplings $g_{\gamma K^* \kappa}^0 / g_{\gamma K^* \kappa}^c$ is -2 in this limit just as in the case of $g_{\gamma K K^*}^0 / g_{\gamma K K^*}^c$, which is close to -1.53 in nature but takes -2 in the SU(3) limit. The coupling constant β_A can be estimated from the observed value of $\Gamma(a_0 \rightarrow \gamma\gamma)$, which leads to $\beta_A = 0.72 \text{ GeV}^{-1}$ [10]. Here we use $M(\kappa) = 900 \text{ MeV}$ and $\Gamma(\kappa) = 550 \text{ MeV}$.

For the couplings of scalar mesons with octet baryons, we again use the values of the Nijmegen potential [8], which gives

$$\begin{aligned}g_{\kappa N \Lambda} &\sim -8.3 \quad (\text{NSC97a}), \\ g_{\kappa N \Lambda} &\sim -10.0 \quad (\text{NSC97f}).\end{aligned}\quad (17)$$

However, it should be mentioned that the above values are obtained with $M(\kappa) = 880$ MeV. Also in Ref. [8], it was stressed that the structure of the scalar mesons is crucial for the central YN potential and the above values are obtained with assuming that the scalar mesons are close to $\bar{q}q$ state. With this caveat in mind, we use the above values just as a guide for the couplings involving the κ meson. Our numerical results show that the κ meson exchange is suppressed and the uncertainties of κ meson coupling constants are not crucial in K^* photoproduction. Collecting the κ meson coupling constants, we have

$$\begin{aligned} |g_{\gamma K^* \kappa}^c g_{\kappa N \Lambda}| &= (1.0 \sim 1.2) e \text{ GeV}^{-1}, \\ g_{\gamma K^* \kappa}^0 g_{\kappa N \Lambda} &= -2 g_{\gamma K^* \kappa}^c g_{\kappa N \Lambda}. \end{aligned} \quad (18)$$

In fact, the phase of $g_{\gamma K^* \kappa}^c g_{\kappa N \Lambda}$ cannot be fixed at this stage. However, since the κ exchange contribution is small, the phase of the above coupling constants is hard to be distinguished in K^* photoproduction. The production amplitude reads

$$\mathcal{M}^{\mu\nu} = -\frac{2g_{\gamma K^* \kappa} g_{\kappa N Y}}{(k-q)^2 - (M_\kappa - i\Gamma_\kappa/2)^2} (k \cdot q g^{\mu\nu} - k^\nu q^\mu), \quad (19)$$

where $g_{\gamma K^* \kappa} = g_{\gamma K^* \kappa}^c$ for the reaction (I) and $g_{\gamma K^* \kappa}^0$ for the reaction (II).

C. *s*-channel diagrams

The *s*-channel diagrams shown in Fig. 1(b) can contain the intermediate nucleon as well as nucleon resonances. The purpose of this work is to investigate the main production mechanisms which should be well understood before studying the nucleon resonances. In this work, therefore, we consider only the intermediate nucleon state postponing the inclusion of nucleon resonances to a future study as it requires more information or assumptions. The consequences of limiting the intermediate state to the nucleon will be discussed later.

The amplitude of the *s*-channel nucleon term can be calculated from $\mathcal{L}_{K^* N \Lambda}$ of Eq. (4) and

$$\mathcal{L}_{\gamma N N} = -e \bar{N} \left[\gamma_\mu A^\mu \frac{1 + \tau_3}{2} - \frac{1}{2M_N} (\kappa_s^N + \kappa_v^N \tau_3) \sigma_{\mu\nu} \partial^\nu A^\mu \right] N, \quad (20)$$

where the isoscalar and isovector anomalous magnetic moments of the nucleon are $\kappa_s^N = -0.06$ and $\kappa_v^N = 1.85$. Then the production amplitude is obtained as

$$\mathcal{M}_N^{\mu\nu} = \frac{e}{(k+p)^2 - M_N^2} \Gamma_{K^* N \Lambda}^\nu(q) (\not{k} + \not{p} + M_N) \Gamma_{\gamma N}^\mu(k), \quad (21)$$

where

$$\Gamma_{\gamma N}^\mu(k) = \gamma^\mu Q_N + \frac{i\kappa_N}{2M_N} \sigma^{\mu\nu} k_\nu, \quad (22)$$

with ($Q_p = +1$, $\kappa_p = 1.79$) for the reaction (I) and ($Q_n = 0$, $\kappa_n = -1.91$) for the reaction (II).

D. *u*-channel diagrams

For the *u*-channel diagrams of Fig. 1(c), we consider intermediate hyperons including $\Lambda(1116)$, $\Sigma(1193)$, and $\Sigma^*(1385)$. The diagrams with the intermediate octet hyperons can

be calculated with

$$\mathcal{L}_{\gamma\Lambda\Lambda} = \frac{e\kappa_\Lambda}{2M_N} \bar{\Lambda} \sigma_{\mu\nu} \partial^\nu A^\mu \Lambda, \quad (23)$$

$$\mathcal{L}_{\gamma\Sigma\Lambda} = \frac{e\mu_{\Sigma\Lambda}}{2M_N} \bar{\Sigma}^0 \sigma_{\mu\nu} \partial^\nu A^\mu \Lambda + \text{H.c.}, \quad (24)$$

where $\kappa_\Lambda = -0.61$ and $\mu_{\Sigma\Lambda} = 1.62 \pm 0.08$. This leads to

$$\begin{aligned} \mathcal{M}_\Lambda^{\mu\nu} &= \eta_\Lambda \frac{e}{(p-q)^2 - M_\Lambda^2} \Gamma_{\gamma\Lambda}^\mu(k) (\not{p} - \not{q} + M_\Lambda) \Gamma_{K^*N\Lambda}^\nu(q), \\ \mathcal{M}_\Sigma^{\mu\nu} &= \eta_\Sigma \frac{e}{(p-q)^2 - M_\Sigma^2} \Gamma_{\Sigma\Lambda}^\mu(k) (\not{p} - \not{q} + M_\Sigma) \Gamma_{K^*N\Sigma}^\nu(q), \end{aligned} \quad (25)$$

where

$$\begin{aligned} \Gamma_{\gamma\Lambda}^\mu(k) &= \frac{i\kappa_\Lambda}{2M_N} \sigma^{\mu\nu} k_\nu, \\ \Gamma_{\Sigma\Lambda}^\mu(k) &= \frac{i\mu_{\Sigma\Lambda}}{2M_N} \sigma^{\mu\nu} k_\nu, \end{aligned} \quad (26)$$

with $\eta_\Lambda = 1$ for the reactions (I) and (II), and $\eta_\Sigma = 1, -1$ for the reaction (I) and (II), respectively, which comes from the isospin factors. The vertex function $\Gamma_{K^*N\Lambda}^\nu(q)$ was given before and $\Gamma_{K^*N\Sigma}^\nu(q)$ has the same structure but with [8]

$$\begin{aligned} g_{K^*N\Sigma} &= -2.46, & \kappa_{K^*N\Sigma} &= -0.47 & \text{(NSC97a),} \\ g_{K^*N\Sigma} &= -3.52, & \kappa_{K^*N\Sigma} &= -1.14 & \text{(NSC97f).} \end{aligned} \quad (27)$$

In order to compute the contribution from the intermediate $\Sigma^*(1385)$, we need to know the interactions $\mathcal{L}_{K^*N\Sigma^*}$ and $\mathcal{L}_{\gamma\Lambda\Sigma^*}$. The general form for $\mathcal{L}_{K^*N\Sigma^*}$ is written as

$$\begin{aligned} \mathcal{L}_{K^*N\Sigma^*} &= -i \frac{f_{K^*N\Sigma^*}^{(1)}}{M_{K^*}} \bar{K}^*_{\mu\nu} \bar{\Sigma}^{*\mu} \cdot \boldsymbol{\tau} \gamma^\nu \gamma_5 N - \frac{f_{K^*N\Sigma^*}^{(2)}}{M_{K^*}} \bar{K}^*_{\mu\nu} \bar{\Sigma}^{*\mu} \cdot \boldsymbol{\tau} \gamma_5 \partial^\nu N \\ &\quad + \frac{f_{K^*N\Sigma^*}^{(3)}}{M_{K^*}} \partial^\nu \bar{K}^*_{\mu\nu} \bar{\Sigma}^{*\mu} \cdot \boldsymbol{\tau} \gamma_5 N + \text{H.c.}, \end{aligned} \quad (28)$$

which follows from the fact that this is an interaction of $J^P = \frac{3}{2}^+ \rightarrow \frac{1}{2}^+ + 1^-$. Thus we have, in general, three independent couplings. However their values are poorly known and we use the SU(3) symmetry relations to estimate the couplings. (See, e.g., Ref. [11].) By making use of the quark model prediction and SU(3) flavor symmetry we obtain

$$f_{K^*N\Sigma^*}^{(1)} = -\frac{1}{\sqrt{6}} \frac{M_{K^*}}{M_\rho} f_{\rho N\Delta}^{(1)} = -2.6, \quad (29)$$

with $f_{\rho N\Delta}^{(1)} = 5.5$ [12, 13]. The other couplings are unknown and we do not consider the terms containing $f_{K^*N\Sigma^*}^{(2)}$ and $f_{K^*N\Sigma^*}^{(3)}$ [13].

The Lagrangian for $\gamma\Lambda\Sigma^*$ interaction has the same structure as $\mathcal{L}_{K^*N\Sigma^*}$ of Eq. (28). Since the photon is massless, the number of independent couplings is reduced to 2 and the interaction can be written as

$$\mathcal{L}_{\gamma\Lambda\Sigma^*} = \frac{ieg_1}{2M_N} \bar{\Sigma}^*_{\mu} \gamma_\nu \gamma_5 \Lambda F^{\mu\nu} + \frac{eg_2}{4M_N^2} \bar{\Sigma}^*_{\mu} \gamma_5 \partial_\nu \Lambda F^{\mu\nu} + \text{H.c.}, \quad (30)$$

which leads to the decay width as

$$\begin{aligned}\Gamma(\Sigma^* \rightarrow \Lambda\gamma) = & \frac{p_\gamma^3}{48\pi M_{\Sigma^*}^2} \left(\frac{e}{2M_N} \right)^2 \left\{ \left[g_1(3M_{\Sigma^*} + M_\Lambda) - g_2 \frac{M_{\Sigma^*}}{2M_N} (M_{\Sigma^*} - M_\Lambda) \right]^2 \right. \\ & \left. + 3 \left[g_1 - g_2 \frac{M_{\Sigma^*}}{2M_N} \right]^2 (M_{\Sigma^*} - M_\Lambda)^2 \right\},\end{aligned}\quad (31)$$

and the $E2/M1$ ratio as [14]

$$R_{EM} = E2/M1 = -\frac{M_{\Sigma^*} - M_\Lambda}{2M_N} \frac{g_1 - g_2 M_{\Sigma^*}/(2M_N)}{g_1(3M_{\Sigma^*} + M_\Lambda)/(2M_N) - g_2 M_{\Sigma^*}(M_{\Sigma^*} - M_\Lambda)/(2M_N)^2}. \quad (32)$$

The recent CLAS experiment puts a constraint on the radiative decay width of $\Gamma(\Sigma^* \rightarrow \Lambda\gamma)$ as [15]

$$\Gamma(\Sigma^* \rightarrow \Lambda\gamma) = 479 \pm 120 {}^{+81}_{-100} \text{ keV}. \quad (33)$$

Together with the chiral quark model prediction on the $E2/M1$ ratio for this radiative decay, $R_{EM} = -2.0\%$ [16], we obtain

$$g_1 = 3.78, \quad g_2 = 3.18. \quad (34)$$

The production amplitude reads

$$\mathcal{M}_{\Sigma^*}^{\mu\nu} = \eta_{\Sigma^*} \frac{e}{(p - q)^2 - M_{\Sigma^*}^2} \Gamma_{\Sigma^*\Lambda}^{\mu\beta}(k, p') \Delta_{\beta\alpha}(\Sigma^*, p - q) \Gamma_{K^*N\Sigma^*}^{\nu\alpha}(q), \quad (35)$$

where $\eta_{\Sigma^*} = 1$ for the reaction (I), $\eta_{\Sigma^*} = -1$ for the reaction (II), and

$$\begin{aligned}\Gamma_{K^*N\Sigma^*}^{\nu\alpha}(q) &= \frac{f_{K^*N\Sigma^*}^{(1)}}{M_{K^*}} \gamma_\delta \gamma_5 (q^\alpha g^{\nu\delta} - q^\delta g^{\nu\alpha}), \\ \Gamma_{\Sigma^*\Lambda}^{\mu\beta}(k, p') &= \left\{ \frac{g_1}{2M_N} \gamma_\nu \gamma_5 + \frac{g_2}{4M_N^2} p'_\nu \gamma_5 \right\} (k^\beta g^{\mu\nu} - k^\nu g^{\mu\beta}).\end{aligned}\quad (36)$$

The spin-3/2 Rarita-Schwinger propagator for the resonance R with momentum p contains

$$\Delta_{\mu\nu}(R, p) = (\not{p} + M_R) \left(-g_{\mu\nu} + \frac{1}{3} \gamma_\mu \gamma_\nu + \frac{1}{3M_R} (\gamma_\mu p_\nu - \gamma_\nu p_\mu) + \frac{2}{3M_R^2} p_\mu p_\nu \right). \quad (37)$$

The decay width is incorporated by replacing $M_R \rightarrow M_R - i\Gamma_R/2$ in the propagator. We use $M_{\Sigma^*} = 1385$ MeV and $\Gamma_{\Sigma^*} = 37$ MeV.

E. Contact diagram

Since the $K^*N\Lambda$ interaction contains a derivative coupling, there exists a contact diagram for the charged K^* vector meson photoproduction. Inclusion of this diagram is essential to satisfy the gauge-invariance condition. By minimal substitution, from the Lagrangian (4), we have

$$\mathcal{L}_{\gamma K^*N\Lambda} = -i \frac{eg_{K^*N\Lambda}\kappa_{K^*N\Lambda}}{2M_N} \bar{\Lambda} \sigma^{\mu\nu} A_\nu K_\mu^{*-} p + \text{H.c.}, \quad (38)$$

which gives the contact diagram of Fig. 1(d). The corresponding amplitude is given by

$$\mathcal{M}_C^{\mu\nu} = -\frac{ieg_{K^*N\Lambda}\kappa_{K^*N\Lambda}}{2M_N} \sigma^{\mu\nu}. \quad (39)$$

F. Form factors

The form factors are included to dress the vertices of the diagrams. For the form factors of t -channel exchanges, F_{K^*} , F_K , and F_κ , we use the form of

$$F_M(p^2) = \frac{\Lambda^2 - M_{\text{ex}}^2}{\Lambda^2 - p^2}, \quad (40)$$

where M_{ex}^2 and p^2 are the mass and momentum squared of the exchanged particle. The form factor is multiplied to each vertex, and each diagram contains two powers of the form factor.

The s - and u -channel diagrams have the form factor, F_N , F_Λ , F_Σ , and F_{Σ^*} , in the form of [17]

$$F_B(p^2) = \left(\frac{n\Lambda^4}{n\Lambda^4 + (p^2 - M_{\text{ex}}^2)^2} \right)^n, \quad (41)$$

which becomes the Gaussian form as $n \rightarrow \infty$. We take $n = 1$ but the results with $n \rightarrow \infty$ will also be discussed.

It is well-known that introducing the form factors that depend on the momentum and mass of the exchanged particle violates the charge conservation condition, $k_\mu \mathcal{M}^{\mu\nu} = 0$ unless the production amplitude is transverse by itself. For example, in the reaction of $\gamma p \rightarrow K^{*+} \Lambda$, the t -channel K^* exchange, s -channel nucleon term, and the contact term separately violate the charge-conservation condition but their sum does not. Having different form factor at each channel clearly makes the sum violate the charge conservation. Various methods to restore the charge-conservation condition have been developed [18, 19, 20, 21]. In this work, following Ref. [21], we take the common form factor for the t -channel K^* exchange, s -channel nucleon term, and the contact term as

$$F = 1 - (1 - F_{K^*})(1 - F_N). \quad (42)$$

In the case of $\gamma n \rightarrow K^{*0} \Lambda$, each production amplitude is transverse. Thus the charge-conservation condition is satisfied even with the form factors and no prescription like Eq. (42) is necessary.

III. RESULTS

Before we present our numerical results, the cutoff parameters should be fixed. We use the total cross section for $\gamma p \rightarrow K^{*+} \Lambda$ reported in Ref. [5] to constrain the cutoff parameters of the form factors. The observed total cross section data show that the cross section has the maximum near the threshold and then decreases as the energy increases. This behaviour is observed in the model of spin-0 meson exchanges, while the spin-1 meson exchange makes the total cross section increase with the energy since the total cross section in the t -channel exchange model scales as $\sigma \sim s^{J-1}$, where J is the spin of the exchanged particle in t -channel. In our case, the charged K^* production contains the K^* vector meson exchange and, as a result, it gives an increasing total cross section with the energy. This is shown by the dot-dashed line of Fig. 2(a), which is obtained with the cutoff $\Lambda_{K^*} = 1.1$ GeV. (See below for the other cutoff parameters.) However, this is not consistent with the experimental observation reported by Ref. [5], which means that the K^* exchange contribution should be suppressed. In fact, the contribution from the higher-spin meson exchanges can be modified

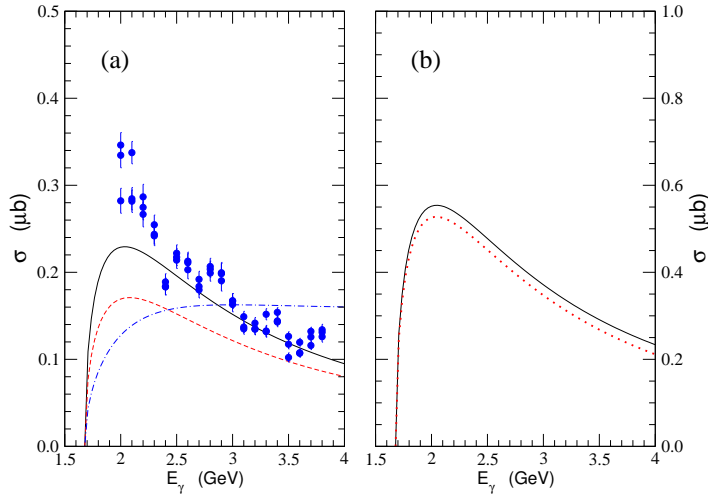


FIG. 2: (color online). Total cross section (a) for $\gamma p \rightarrow K^{*+} \Lambda$ and (b) for $\gamma n \rightarrow K^{*0} \Lambda$. In (a), the solid line is obtained with $\Lambda_{K^*} = 0.9$ GeV, while the dashed and dot-dashed lines are obtained with $\Lambda_{K^*} = 1.0$ and 1.1 GeV, respectively. In (b), the solid line is the full calculation and the dotted line is obtained from the t -channel K exchange alone. The experimental data are from Ref. [5].

by reggeizing the production amplitude. In this exploratory work, however, in order to avoid additional complexity, we simply suppressed the K^* exchange by employing a soft form factor with $\Lambda_{K^*} = 0.9$ GeV.

Shown in Fig. 2 are the total cross sections for $\gamma p \rightarrow K^{*+} \Lambda$ (left panel) and $\gamma n \rightarrow K^{*0} \Lambda$ (right panel). These results are obtained with the (NSC97a) values for the K^* and κ couplings. The solid lines are obtained with $\Lambda_{K^*} = 0.9$ GeV and $\Lambda_K = \Lambda_\kappa = 1.1$ GeV, while the s - and u -channel form factors have $\Lambda = 0.9$ GeV [13]. This gives a good fit to the measured total cross sections except the near-threshold region. In the left panel we also give the results obtained with $\Lambda_{K^*} = 1.0$ GeV (dotted line) and with $\Lambda_{K^*} = 1.1$ GeV (dot-dashed line) while keeping the other cutoff parameters. The decrease of the total cross section by changing $\Lambda_{K^*} = 0.9$ GeV to $\Lambda_{K^*} = 1.0$ GeV shows the destructive interference between the K exchange and K^* exchange. With $\Lambda_{K^*} = 1.1$ GeV, the vector meson exchange starts to dominate and the total cross section shows the behavior expected from the vector meson exchange model. With $\Lambda_{K^*} = 0.9$ GeV, the K^* vector meson exchange is suppressed and, in fact, the kaon exchange dominates the reaction.

The K meson exchange dominance can be also seen in the neutral K^* production shown in Fig. 2(b). The vector meson exchange does not contribute to this reaction and Fig. 2(b) shows the behavior expected from the pseudoscalar meson exchange model. One can clearly see from the dotted line that the cross section is almost dominated by the K exchange. Figure 2 also shows that the cross section for the neutral K^* photoproduction is larger than that for the charged K^* photoproduction. This can be understood by the dominance of K exchange and the ratio of $|g_{\gamma K K^*}^0/g_{\gamma K K^*}^c| \simeq 1.53$.

A close inspection of our results for total cross sections with the data of Ref. [5] shows that our model can describe the charged K^* meson production process at large energies,

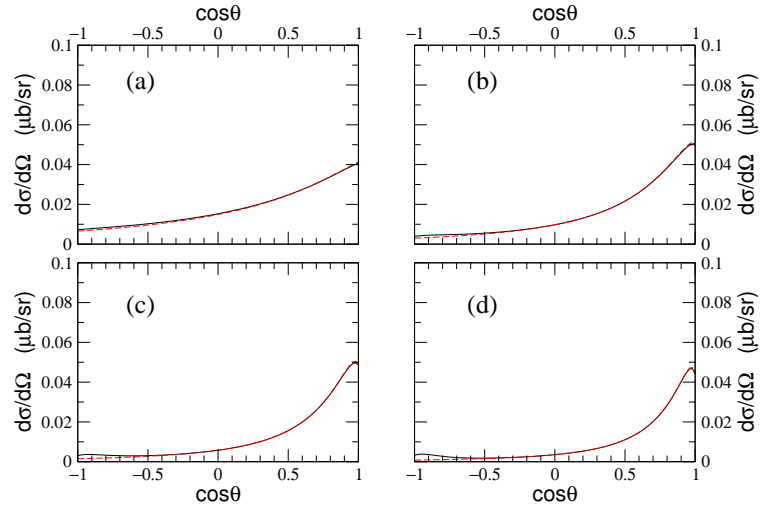


FIG. 3: (color online). Differential cross sections for $\gamma p \rightarrow K^* \Lambda$ at E_γ = (a) 2.0 GeV, (b) 2.5 GeV, (c) 3.0 GeV, and (d) 3.5 GeV. The solid lines are the full calculation and dashed lines are for the K meson exchange alone.

$E_\gamma > 2.3$ GeV. But there is discrepancy between the two at lower energies. This may be ascribed to limiting the s - and u -channel diagrams to the intermediate lowest octet and decuplet baryons. We expect that the low energy behavior can be improved by including the nucleon resonances lying near the $K^* \Lambda$ threshold.

The differential cross sections for the charged and neutral K^* photoproduction are given in Figs. 3 and 4, respectively, at four photon energies, $E_\gamma = 2.0, 2.5, 3.0$, and 3.5 GeV. They are given as functions of the scattering angle θ , which is defined as the angle between the photon beam and the outgoing K^* vector meson in the center-of-mass frame. In both cases, we have a forward peak as a result of the K -exchange dominance. The effects of the other production amplitudes can be barely seen only at large scattering angle region. The contribution coming from the scalar κ meson exchange is suppressed in the considered energy region. We have varied the κ meson couplings including the phase around the values of Eq. (18), but the changes are hard to be seen.

We have also employed the Gaussian form factor by taking the limit of $n \rightarrow \infty$ in Eq. (41) and found no significant difference in the differential cross sections. (A counter-example can be found, e.g., in Refs. [22].) The only difference could be seen in the backward scattering region, $\cos \theta \leq -0.5$, because the form factor with $n \rightarrow \infty$ suppresses the differential cross section at large scattering angles more than that with $n = 1$. However, it is hard to distinguish them.

Next we consider the spin asymmetries. Since contributions from the baryon resonances are expected to be seen mostly in the backward scattering angles, $\cos \theta < 0$, here we focus on the spin asymmetries in the range $\cos \theta \geq -0.5$. Because of the K -exchange dominance, the single asymmetries for photon, nucleon, and Λ are close to zero for forward scattering angles. As an example, in Fig. 5(a), the single photon asymmetry is shown which is defined

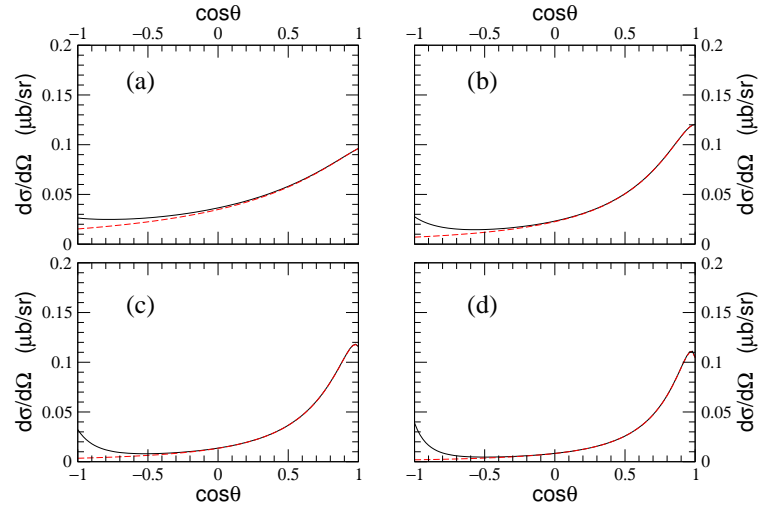


FIG. 4: (color online). Differential cross sections for $\gamma n \rightarrow K^{*0}\Lambda$ at $E_\gamma = 2.0$ GeV, (b) 2.5 GeV, (c) 3.0 GeV, and (d) 3.5 GeV. The solid lines are the full calculation and dashed lines are for the K meson exchange alone.

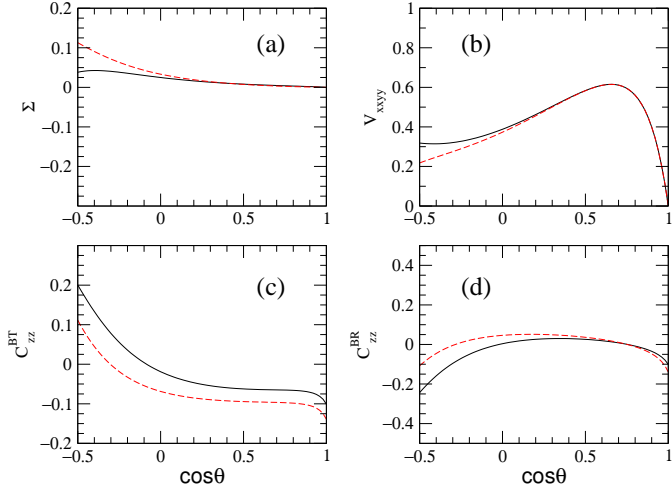


FIG. 5: (color online). Spin asymmetries (a) Σ , (b) V_{xyxy} , (c) C_{zz}^{BT} , and (d) C_{zz}^{BR} for $\gamma p \rightarrow K^{*+}\Lambda$ (solid lines) and for $\gamma n \rightarrow K^{*0}\Lambda$ (dashed lines) at $E_\gamma = 3.0$ GeV.

as

$$\Sigma = \frac{\sigma^{\parallel} - \sigma^{\perp}}{\sigma^{\parallel} + \sigma^{\perp}}, \quad (43)$$

where σ^{\parallel} (σ^{\perp}) is the differential cross section produced by a photon linearly polarized along the \hat{x} and (\hat{y}) axis in the CM frame. Also given in Fig. 5 are the tensor polarization

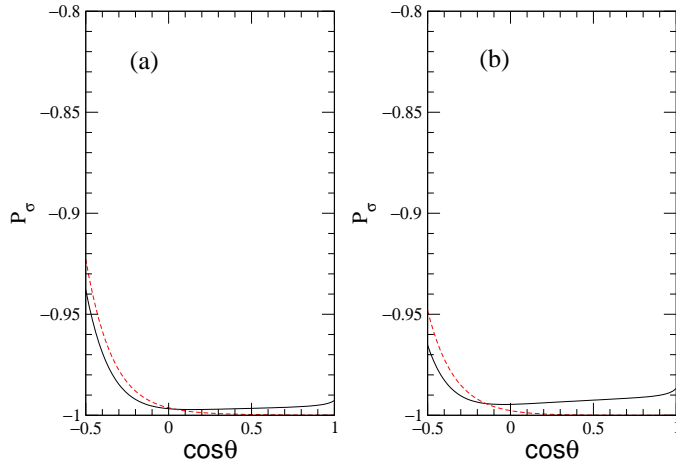


FIG. 6: (color online). Parity asymmetry P_σ (a) for $\gamma p \rightarrow K^{*+}\Lambda$ and (b) for $\gamma n \rightarrow K^{*0}\Lambda$ at $E_\gamma = 3.0$ GeV. The solid lines are the full calculation while the dashed lines are obtained without the κ exchange.

asymmetry V_{xxyy} of the K^* vector meson, beam-target double asymmetry C_{zz}^{BT} , and beam-recoil double asymmetry C_{zz}^{BR} . The solid lines in Fig. 5 are the results for $\gamma p \rightarrow K^{*+}\Lambda$ and the dashed lines for $\gamma n \rightarrow K^{*0}\Lambda$. The definition for these asymmetries and the coordinate system can be found, e.g., in Refs. [23].

Another interesting feature of K^* production reaction is that the scalar $\kappa(900)$ meson exchange is allowed. In fact, since the κ exchange is a natural-parity exchange, while the K meson exchange is an unnatural-parity exchange, the relative strength of them can be estimated by measuring the parity asymmetry defined as [24, 25]

$$P_\sigma \equiv \frac{\sigma^N - \sigma^U}{\sigma^N + \sigma^U} = 2\rho_{1-1}^1 - \rho_{00}^1, \quad (44)$$

where σ^N and σ^U are the contributions of natural and unnatural parity exchanges to the cross section, and the asymmetry P_σ can be expressed in terms of the K^* density matrix elements. From its definition, it can be easily found that $P_\sigma \rightarrow -1$ for the K exchange, while it becomes $+1$ for K^* and κ exchanges. The reaction $\gamma n \rightarrow K^{*0}\Lambda$, where the K^* exchange does not contribute, is a good place to estimate the relative strength between the K exchange and the κ exchange. In our model, however, the contribution from the κ exchange is suppressed and P_σ is very close to -1 as can be seen from Fig. 6. (The photon polarization asymmetry Σ_V [25] also gives the similar results.)

IV. SUMMARY

We have investigated photoproduction mechanisms of $K^*\Lambda$ off the nucleon targets. Our calculation includes the t -channel strange meson exchanges as well as the s - and u -channel intermediate nucleon and hyperon diagrams. Baryon resonances, which are predicted to

have sizable couplings with $K^*\Lambda$ [2], can also participate in the reaction. Our calculation thus can provide background production mechanisms to investigate such resonances in $K^*\Lambda$ photoproduction. We have found that the K -meson exchange dominates both the charged and neutral K^* photoproduction, which leads to sharp peaks in the differential cross sections at forward scattering angles. Because of the K -exchange dominance, the total cross sections for the neutral K^* photoproduction is found to be larger than those for the charged K^* photoproduction. Comparison with the experimental data of Ref. [5] shows that the inclusion of baryon resonances can improve our model prediction at lower energies close to the threshold.

As a test for our model, we have made several predictions on the spin asymmetries which can be measured at current experimental facilities. One advantage of K^* photoproductions over K photoproductions is that it allows the κ -meson exchange whose existence and properties are still under debate. However, within our model, we found that the contribution from the $\kappa(900)$ meson exchange is suppressed and can hardly be seen in the reaction of $K^*\Lambda$ photoproduction. Therefore, the parity asymmetry P_σ , which can distinguish the relative strength between the κ and K exchanges especially in the neutral K^* production, is found to be $P_\sigma \simeq -1$ due to the K -meson exchange dominance. Measurement of those spin asymmetries would be helpful to test the reaction mechanisms of K^* photoproduction such as the dominance of the K meson exchange.

Acknowledgments

We are grateful to L. Guo, K. Hicks, T.-S.H. Lee, and K. Nakayama for fruitful discussions and encouragements. Y.O. was supported by Forschungszentrum-Jülich, contract No. 41445282 (COSY-058).

- [1] S. Capstick and W. Roberts, *Prog. Part. Nucl. Phys.* **45**, S241 (2000).
- [2] S. Capstick and W. Roberts, *Phys. Rev. D* **58**, 074011 (1998).
- [3] Y. Oh, A. I. Titov, and T.-S. H. Lee, *Phys. Rev. C* **63**, 025201 (2001).
- [4] I. Hleiqawi and K. Hicks for the CLAS Collaboration, *nucl-ex/0512039*.
- [5] L. Guo and D. P. Weygand for the CLAS Collaboration, *hep-ex/0601010*.
- [6] Q. Zhao, J. S. Al-Khalili, and C. Bennhold, *Phys. Rev. C* **64**, 052201 (2001).
- [7] Y. Oh, H. Kim, and S. H. Lee, *Nucl. Phys.* **A745**, 129 (2004).
- [8] V. G. J. Stoks and Th. A. Rijken, *Phys. Rev. C* **59**, 3009 (1999); Th. A. Rijken, V. G. J. Stoks, and Y. Yamamoto, *Phys. Rev. C* **59**, 21 (1999).
- [9] R. L. Jaffe, *Phys. Rev. D* **15**, 267 (1977); J. Weinstein and N. Isgur, *Phys. Rev. D* **41**, 2236 (1990); F. E. Close, Y. L. Dokshitzer, V. N. Gribov, V. A. Khoze, and M. G. Ryskin, *Phys. Lett. B* **319**, 291 (1993); M. Ishida, *AIP Conf. Proc.* **688**, 18 (2004); C. Amsler and N. A. Törnqvist, *Phys. Rep.* **389**, 61 (2004). D. V. Bugg, *Phys. Rep.* **397**, 257 (2004).
- [10] D. Black, M. Harada, and J. Schechter, *Phys. Rev. Lett.* **88**, 181603 (2002).
- [11] Y. Oh and H. Kim, *Phys. Rev. D* **70**, 094022 (2004).
- [12] H. Kammano and M. Arima, *Phys. Rev. C* **69**, 025206 (2004).
- [13] Y. Oh, K. Nakayama, and T.-S. H. Lee, *Phys. Rep.* **423**, 49 (2006).
- [14] S. Nozawa, B. Blankleider, and T.-S. H. Lee, *Nucl. Phys.* **A513**, 459 (1990).

- [15] CLAS Collaboration, S. Taylor *et al.*, Phys. Rev. C **71**, 054609 (2005).
- [16] G. Wagner, A. J. Buchmann, and A. Faessler, Phys. Rev. C **58**, 1745 (1998).
- [17] B. C. Pearce and B. K. Jennings, Nucl. Phys. **A528**, 655 (1991).
- [18] K. Ohta, Phys. Rev. C **40**, 1335 (1989).
- [19] H. Haberzettl, Phys. Rev. C **56**, 2041 (1997).
- [20] H. Haberzettl, C. Bennhold, T. Mart, and T. Feuster, Phys. Rev. C **58**, 40 (1998).
- [21] R. M. Davidson and R. Workman, Phys. Rev. C **63**, 025210 (2001).
- [22] Y. Oh, T. Song, and S. H. Lee, Phys. Rev. C **63**, 034901 (2001); Y. Oh, T. Song, S. H. Lee, and C.-Y. Wong, J. Korean Phys. Soc. **43**, 1003 (2003).
- [23] A. I. Titov, Y. Oh, S. N. Yang, and T. Morii, Phys. Rev. C **58**, 2429 (1998).
- [24] G. Cohen-Tannoudji, Ph. Salin, and A. Morel, Nuovo Cimento **55**, 412 (1968).
- [25] K. Schilling, P. Seyboth, and G. Wolf, Nucl. Phys. **B15**, 397 (1970), **B18**, 332(E) (1970).